1989

Hydrographic Variability of Southeastern United States Shelf and Slope Waters During the Genesis of Atlantic Lows Experiment: Winter 1986

Larry P. Atkinson
Old Dominion University, latkinso@odu.edu

Eiichi Oka
Old Dominion University

Sunny Y. Wu
Old Dominion University

Thomas J. Berger

Jackson O. Blanton

See next page for additional authors

Original Publication Citation

Atkinson, L. P., Oka, E., Wu, S. Y., Berger, T. J., Blanton, J. O., & Lee, T. N. (1989). Hydrographic variability of southeastern United States shelf and slope waters during the genesis of Atlantic lows experiment: Winter 1986. *Journal of Geophysical Research: Oceans, 94*(C8), 10699-10713. doi:10.1029/JC094iC08p10699

JOURNAL OF GEOPHYSICAL RESEARCH, VOL. 94, NO. C8, PAGES 10,699–10,713, AUGUST 15, 1989

Hydrographic Variability of Southeastern United States Shelf and Slope Waters During the Genesis of Atlantic Lows Experiment: Winter 1986

LARRY P. ATKINSON,[1] EIICHI OKA,[1] SUNNY Y. WU,[1] THOMAS J. BERGER,[2] JACKSON O. BLANTON,[3] AND THOMAS N. LEE[4]

Continental shelf waters are particularly responsive to winter storm events mainly because of their shallow depths. Those of the southeastern United States (the South Atlantic Bight (SAB)) are especially responsive because they are broad and shallow. Also, the Gulf Stream serves as a continual source of warm water at the outer boundary. Thus the SAB receives strong meteorological (wind stress and heat loss) and oceanographic (advective) forcing. During the Genesis of Atlantic Lows Experiment (GALE) the response of shelf waters to winter storm events and Gulf Stream forcing was observed. The mean conditions showed a mixed water column with areas of stratification near the coast and at the shelf break. The nearshore area was stratified only during weak offshore winds, and the shelf break area was stratified during southward winds with accompanying onshore Ekman flow. On the inner shelf, advective buoyancy flux was similar in value to heat flux buoyancy and the buoyancy equivalent of wind mixing. Over the shelf break the advective buoyancy flux was 4 times the other forms of buoyancy flux and controlled the observed potential energy variability. A simple box model heat budget used to separate the effect of Gulf Stream eddies and meanders, and Ekman flow and air-sea heat exchange on the shelf heat content showed that the observed heat content variability was caused by intrusion of Gulf Stream water. The intrusions may be caused either by onshore Ekman flow during southward winds or Gulf Stream meander events.

INTRODUCTION

Continental shelf and slope waters along mid-latitude oceanic western margins are greatly influenced by weather. Because these waters are shallow they are readily affected by atmospheric forcing such as heating and cooling and turbulent mixing processes. This process of heating, cooling, and mixing of shelf waters creates varying thermal and density contrasts with adjacent ocean waters, often resulting in front formation [*Garwood et al.*, 1981; *Huh et al.*, 1978, 1984; *Nowlin and Parker*, 1974; *Price et al.*., 1978]. The temperature and density contrast is accentuated off the southeastern United States because the Gulf Stream is constantly supplying warm water. Thus even when offshore Gulf Stream water is cooled, it is replaced by more warm water from the south. The result is that while shelf waters off Georgia and South Carolina cool from 25°–30°C to 5°–10°C, waters just a few kilometers offshore in the Gulf Stream cool only to 20°–25°C. This differential cooling combined with other local processes causes a variety of hydrographic structures.

The hydrographic structures observed over the shelf and slope in the South Atlantic Bight (SAB) were classified by *Atkinson* [1977]. Examples taken from the experiment described in this paper are shown in Figure 1. Over the inner shelf any structure is usually caused by a halocline related to river inflow (Fig. 1*a*). The middle shelf exhibits structure either because of an offshore extension of the coastal halocline or an onshore penetration of the Gulf Stream (Figures 1*a* and 1*b*). The onshore penetration of the Gulf Stream manifests itself during winter as a surface layer of lighter, warmer water overlying denser, colder shelf water (Figure 1*c*). During the summer lighter shelf water overlies denser, saltier Gulf Stream water. Over the outer shelf and shelf break, the Gulf Stream front can exhibit a variety of structures in the winter that are also summarized in this figure. Probably the most common feature in the Gulf Stream front, as identified by isopycnals, isohalines, or isotherms, rising to the surface over the upper slope or shelf break. This simple structure is often made more complex by wind and atmospheric cooling or warming events and the passage of Gulf Stream frontal eddies. The passage of Gulf Stream frontal eddies is the most difficult to identify in hydrographic data, since dome structures can occur for a variety of reasons. Figures 1*b* and 1*d* include the typical signature of a frontal eddy: a cold dome structure that here is 90 km offshore. When examining hydrographic data, the presence of a "cold dome" is often used as evidence of a frontal eddy. Such a feature, however, may also be present from cascading of cooled shelf water over the shelf break [*Stefansson et al.*, 1971], or as will be shown, it may be caused by shelf break or upper slope upwelling. All these processes result in fronts with various characteristics and at various locations over the shelf.

A particularly strong front seems to occur during southward winds accompanying cold air outbreaks. *Oey* [1986, p. 1121] theorized that "Density fronts on the U.S. southeastern continental shelf, during the winter, are formed by (i) breakdown of the shelf-break front by Gulf Stream meanders or strong southward winds or both, (ii) shoreward intrusion of upper Gulf Stream warm water by persistent southward winds, and (iii) mixing of this warm water with continental shelf water cooled by cycles of cold air outbreaks." Oey's model results suggest that three or more winter storms are necessary to promote the development of a mid-shelf front. The mid-shelf front is formed and maintained by the onshore transport of warm Gulf Stream water during southward

[1]Department of Oceanography, Old Dominion University, Norfolk, Virginia.
[2]Science Application International Corporation, Raleigh, North Carolina.
[3]Skidaway Institute of Oceanography, Savannah, Georgia.
[4]Rosenstiel School of Marine and Atmospheric Sciences, University of Miami, Miami, Florida.

Paper number 89JC00488.
0148-0227/89/89JC-00488$05.00

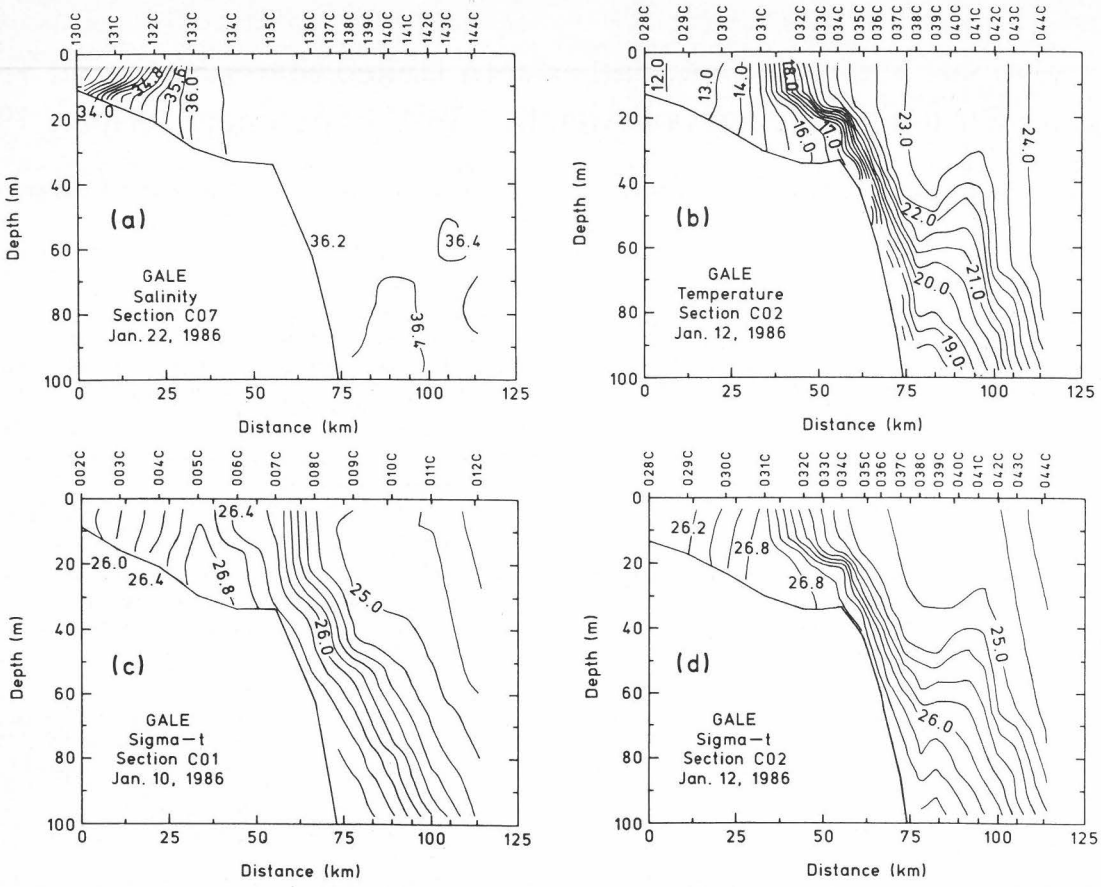

Fig. 1. Examples of various hydrographic structures. (*a*) Inner shelf halocline (section C07 salinity). (*b*) Onshore flow of surface Gulf Stream water (section C02 temperature). (*c*) Simple Gulf Stream front surfacing over outer shelf (section C01 density). (*d*) Doming over upper slope caused by Ekman upwelling, cascading or frontal eddy processes (section C02 density and section C02 temperature).

winds. This balances the offshore transport of colder, denser shelf water via the downward turbulent diffusion of warm water [see *Oey et al.*, 1987, Figure 1]. In addition to the frontal formation, Oey's model suggests transient upwelling over the upper slope during southward winds. This paper reports on observations taken to investigate hydrographic variability during winter storm events and to further test Oey's model. The results confirm the model results published by *Oey* [1986] and *Oey et al.* [1987]. An example of outer shelf front from the Genesis of Atlantic Storms Experiment (GALE) observations is shown in Figure 1*b*. It lies between 50 and 75 km offshore over the upper slope and shelf break.

Rationale for GALE Oceanographic Observations

GALE was a meteorological experiment to study cyclogenesis off the east coast of the United States and the effect of rapid cooling on shelf and Gulf Stream dynamics. An integrated set of oceanographic observations was made off Charleston, South Carolina, during GALE that took full advantage of the meteorological observations. The Charleston area was chosen because it provided the widest shelf in the GALE area and weaker forcing from Gulf Stream interactions. Observation platforms included aircraft, ships, and moorings. The basic ship sampling plan was to repeatedly occupy a transect across the shelf and Gulf Stream off Charleston to observe time and spatial variability before, during, and after storm passage. The Charleston section and mooring are shown in Figure 2. A general description of GALE is given by *Blanton et al.* [1987].

Meteorological Setting

Since GALE was primarily a meteorological study, there is an abundance of such data. The reader is referred to *Blanton et al.* [this issue] and *Bane and Osgood* [this issue] for a more complete description of the meteorology. The air temperature and the across-shelf and alongshelf wind speed at the Savannah River Navigational Light Tower are shown in Figure 3. *Blanton et al.* [this issue] show that winds are coherent over the entire study area. The principal event was the cold air outbreak in late January that was preceded by strong southwestward winds that then changed to eastward. Similar events of less magnitude occurred earlier in the month.

Oceanographic Response

This section describes the variability in the temperature, salinity, and density fields. For reference the mean and standard deviation in the temperature, salinity, and density fields are shown first (Figure 4). The important features to note include the Gulf Stream over the shelf break and upper slope, the strong horizontal gradients over the middle shelf, the reversed vertical temperature gradients over the inner and middle shelf, low-salinity water over the inner shelf, the

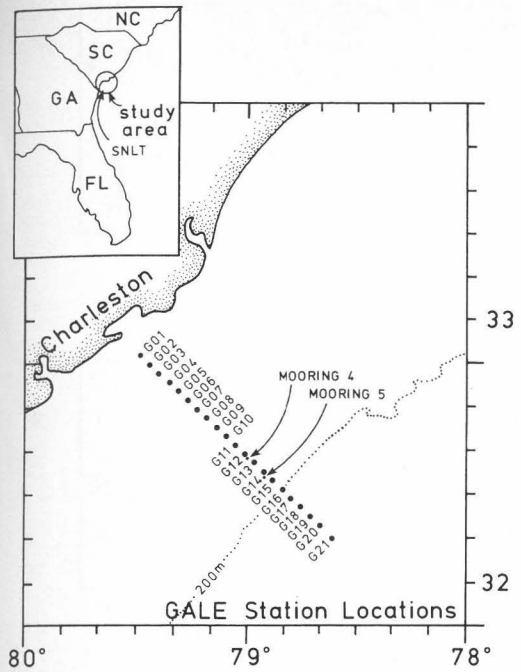

Fig. 2. The GALE study area off South Carolina. The line of stations occupied is shown, as are the locations of the Savannah Navigational Light Tower (SNLT on upper left inset panel) and moorings 4 and 5 off Charleston that are referred to in Figure 3. Moorings 4 and 5 are on the 40- and 75-m isobaths, respectively.

middle shelf density maximum, and indications of upwelling over the upper slope. Temperature variability was highest over the outer shelf because of the Gulf Stream, while salinity variability was highest over the inner shelf because of runoff. Since density is controlled mainly by temperature in this area, the highest density variability was over the shelf break.

The variability of temperature, salinity, and density fields is best discussed by examining the wind, currents, and air temperature (Figure 3) and cross-shelf observations of temperature, salinity, and density (Figures 5–7). Figures of *Lee et al.* [this issue] show satellite-derived sea surface temperatures (SST) with overlayed current vectors. Of particular interest is the shape of the front between the Gulf Stream and shelf waters, the vertical structure over the shelf, and the vertical structure in the Gulf Stream itself. Finally, it must be mentioned that the principal forces at work relevant to oceanographic variability are air-sea heat exchange that occurs throughout the area, wind forcing, meandering of the Gulf Stream front, and passage of frontal eddies along the Gulf Stream front. These latter three forces affect the outer shelf and upper slope more than the inner and middle shelf. Inner and middle shelf currents are wind driven while outer shelf currents follow either the wind or meanders, eddies, and gyres. The notable events in the time series of hydrographic sections are as follows:

January 10–12. During this time, cooling and southward winds caused onshore flow of warm, saline Gulf Stream water to overlie the colder, fresher shelf waters. The doming may be related to upwelling over the upper slope. [*Oey*, 1986]. Isotherms are doming over the upper slope. Alongshore currents at the shelf break were northward and decreasing because of either the decreasing winds or an offshore shift in the Gulf Stream. January 10 marked the time of maximum northward surface currents at the 75-m isobath suggesting an offshore shift in the Gulf Stream. Cross-shelf surface currents at both 40 and 75 m became onshore during this time period while at depth they remained offshore, suggesting that Ekman dynamics are prevailing.

January 14. Outer shelf front structure weakened with offshore winds. A weak front persisted 25 km offshore. The middle shelf density maximum moved inshore. Note that this maximum coincides with the strongest horizontal temperature gradient. Alongshore currents at all depths at both isobaths remained or trended toward northward. Cross-shelf currents at the 40-m isobath switched to offshore at the surface but remained weakly onshore at the 75-m isobath. Near-bottom cross-shelf currents weakened but remained onshore at 40 m and weakened to near zero at 75 m.

January 16. Hydrographic structures over the shelf and slope remained the same during the switch from northward to southward winds. Horizontal gradients remained in place, but the middle shelf density maximum moved offshore about 5 km. Slight doming at 80 m, 80 km from shore, may signal the arrival of a frontal eddy propagating into the area from the south [*Lee et al.*, this issue]. Alongshore currents weakened but remained northward in the upper layer at the 75-m isobath but switched to southward near bottom at 40 m. Cross-shelf currents weakened at the 40-m isobath. Cross-shelf currents at the 75-m isobath were also offshore. The apparent lack of response to southward winds probably was observed because the southward winds had only been present for less than a day; thus the waters had not responded.

January 19. Winds continued weakly southwestward, and the front over the middle shelf (30 km offshore) strengthened and showed evidence of Ekman flow. Alongshore currents were northward at both moorings and all depths although highly variable. Cross-shelf currents at the 45-m isobath shifted from offshore to onshore between January 18 and 19. At the 75-m isobath, surface currents were weak at the surface and bottom but weakening. Onshore movement of the 20°C isotherm suggested onshore movement of the Gulf Stream and doming at 60–100 m, 100 km offshore, is further evidenced for the arrival of the frontal eddy.

January 20. Northeastward winds and a weak cold air outbreak cause the shelf waters to mix. The 20°C isotherm moved eastward, away from the shelf break, and 18°C water moved onshore and upward toward the shelf break. The doming at 100 km persisted, and the 22°C isotherm moved eastward. This pattern of offshore movement of the isotherms and onshore flow of cold water near bottom is typical of eddy passage. Alongshore currents at the 40- and 75-m isobaths remained northward. Cross-shelf currents at the 40-m isobath were offshore in the upper layer and were onshore near bottom. At the 75-m isobath, upper layer currents were offshore. Near-bottom currents at 75 m were onshore.

January 22. Weak northward winds resulted in an estuarinelike nearshore structure, and the Gulf Stream moved offshore. Note the disappearance of 18°C water over the upper slope. Alongshore currents remained northward but were weakening and did become southward near bottom at 75 m. Cross-shelf flow in the upper layer at 40 m were offshore, while in the lower layer they were onshore. At 75 m, cross-shelf currents were offshore at both isobaths.

January 24–25. Strong southwestward winds before the

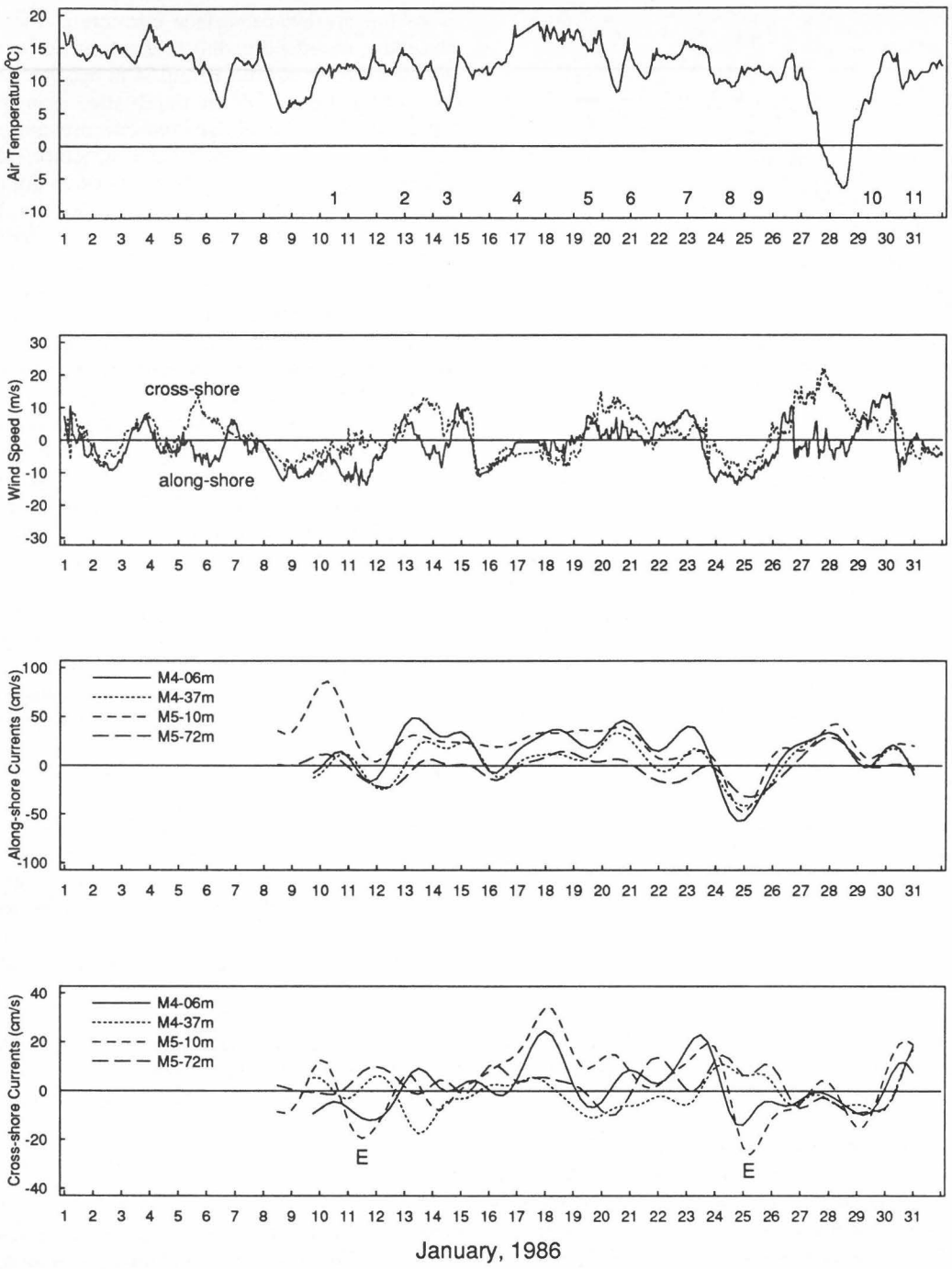

Fig. 3. Time series of air temperature (27 m), alongshore (positive northward) and cross-shelf (positive eastward) wind speed at the Savannah River Navigational Light Tower (SNLT in Figure 2), and alongshore and cross-shelf currents from moorings 4 and 5 (Figure 2). Mooring number and current meter depth are shown. The small E's mark periods of Ekman response: surface onshore flow and bottom times when the shelf break was displaying. Numbers 1 through 11 in the upper panel refer to the time of hydrographic sections shown in Figures 5–7.

major cold air outbreak caused the shelf to be well mixed with strong horizontal gradients over the middle and outer shelf. The 22°C isotherm moved offshore, while isotherms over the outer shelf moved onshore. Alongshore currents rotated from northward to southward during this time reaching peak velocities on January 25. Cross-shelf currents in the surface layer at both moorings and near bottom at 75 m rotated from offshore to onshore with peak onshore velocity on January 25. Cross-shelf currents near bottom were offshore suggesting an Ekman response.

January 29–30. Strong southeastward winds and a cold air outbreak caused onshore flow of Gulf Stream water onto the shelf, formation of a middle shelf front, and possible cascading of dense inner shelf water along the bottom to the shelf break. A temperature-salinity (*T-S*) plot of data from stations 211–217 (Figure 8) shows that at all stations the bottom water was colder and fresher than surface water and the bottom was colder and fresher nearshore. At 40 m, alongshore currents remained northward, against the wind, while cross-shelf currents were onshore at all depths. At 75

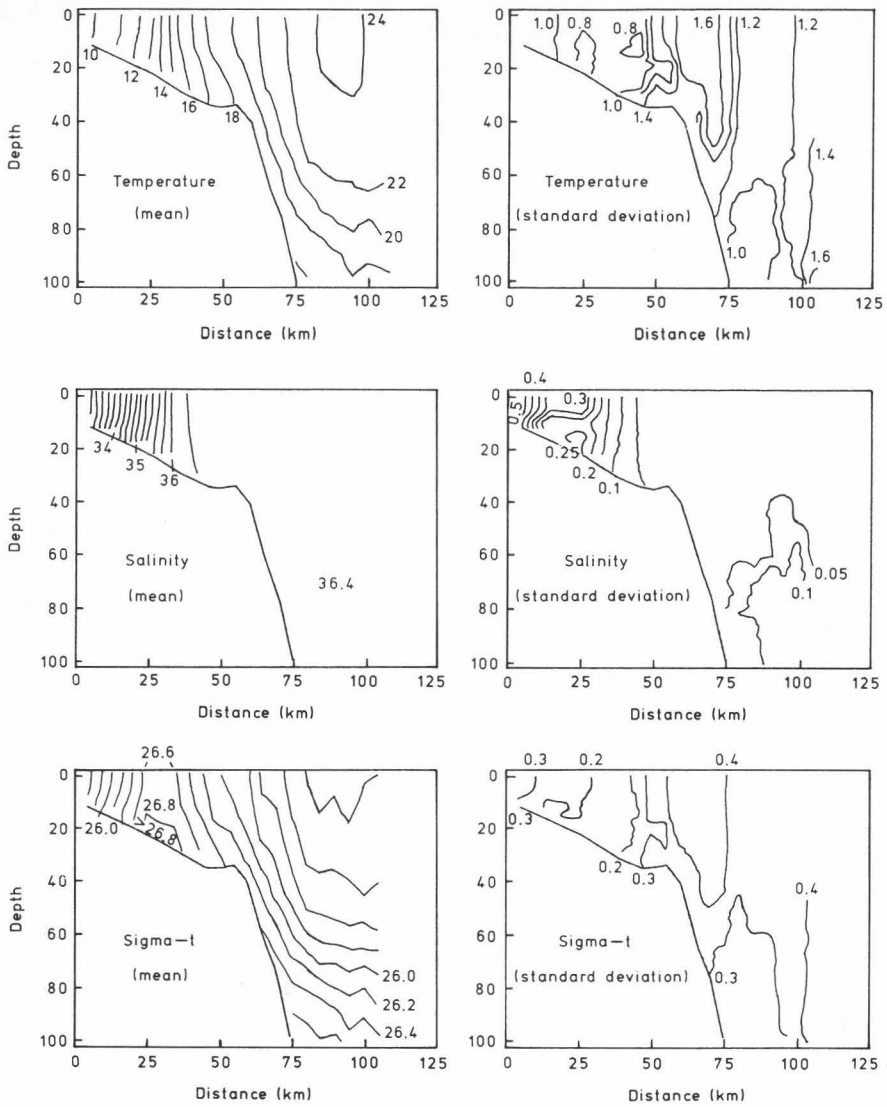

Fig. 4. Mean and standard deviation of temperature, salinity, and density across the shelf off Charleston, South Carolina. Data taken from 11 cross-shelf sections shown in Figures 5–7.

m, alongshore currents were northward and weak, and they weakened with depth. Cross-shelf currents switched to offshore with peak velocities on January 30. The middle shelf density maximum reached 27 σ_t.

Stratification and Mixing Processes

The hydrographic observations shown in the last section shows the variable nature of frontal structures on the shelf. With these data we can now begin to determine the forces that cause the formation and variability of the fronts. It will be shown that stratification of shelf waters depends on the advection of buoyancy from either the near shore or the Gulf Stream and that heat content of shelf waters depends on air-sea heat exchange, wind-induced onshore flow of offshore waters, and onshore flow caused by Gulf Stream meanders.

Potential Energy Variability

The energy required to mix a stratified water column is defined by the potential energy anomaly

$$\mathrm{PE} = \int_{-h}^{0} (\rho_w - \bar{\rho}_w) g z \, dz \qquad (J\ m^{-2}) \tag{1}$$

where z is depth positive up, h is the water depth, ρ_w is the water density, $\bar{\rho}_w$ is the vertically averaged water density, and g is the gravitational acceleration. The time series of potential energy anomaly, hereafter simply called potential energy, for each station (G01 through G21) is shown in Figure 9. The figure is broken into three panels representing inner (top panel), middle (middle panel), and outer shelf stations (lower panel). The inner shelf water column was well mixed at stations G01–G05 except on January 19 and 22, when PE reached maximums because of stratification. The middle shelf PE showed maximums on January 12, 19, and 22–31. The January 12 peak was caused by onshore flow of warm Gulf Stream water in the shelf break region. The maximum on January 19 and 22 was caused by southwest winds, while the one on January 22 may have been caused by minor frontal eddy or meander events. Potential energy over the outer shelf and upper slope was 10 times more during stratification events than inner-middle shelf potential energy,

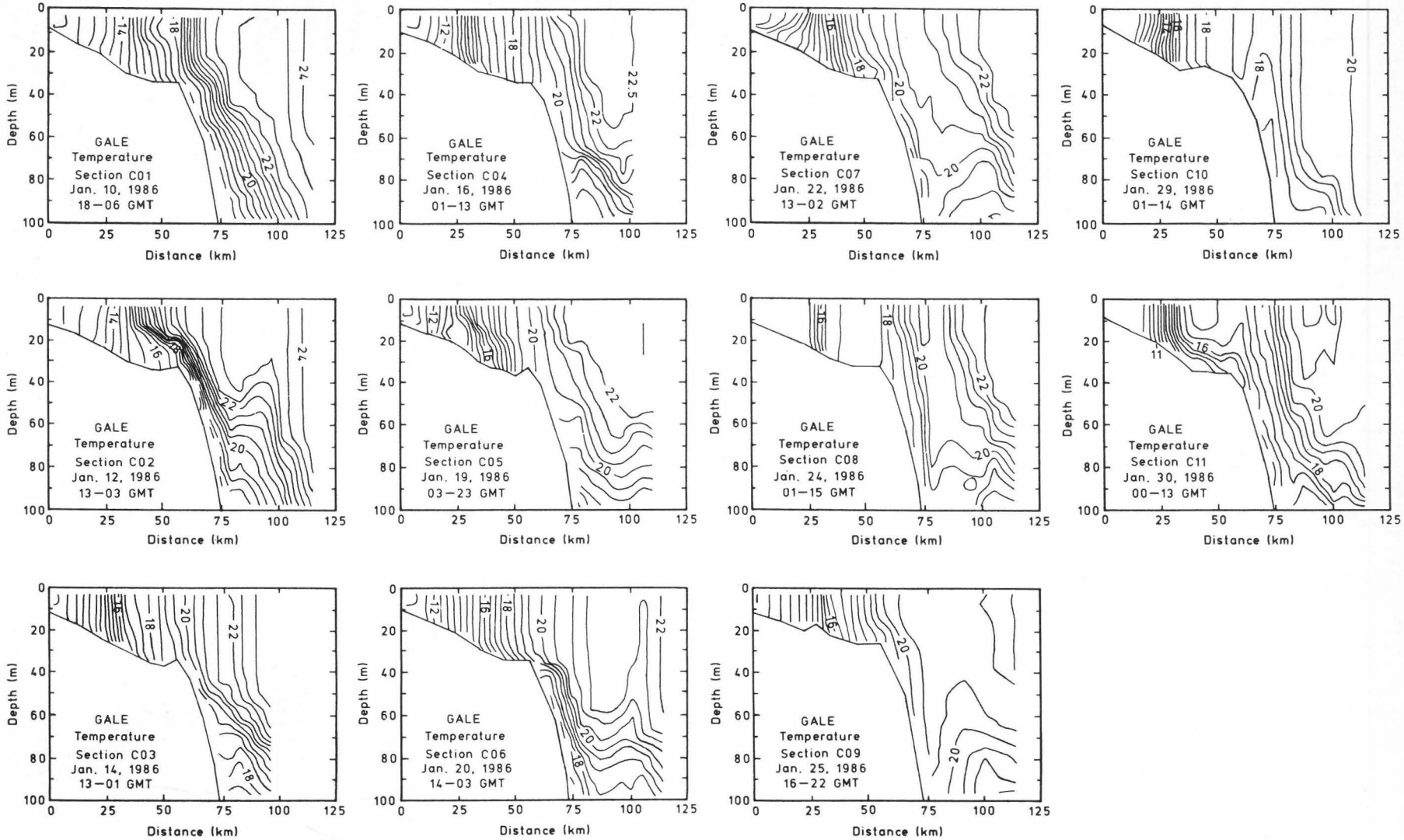

Fig. 5. Cross-shelf sections of temperature off Charleston.

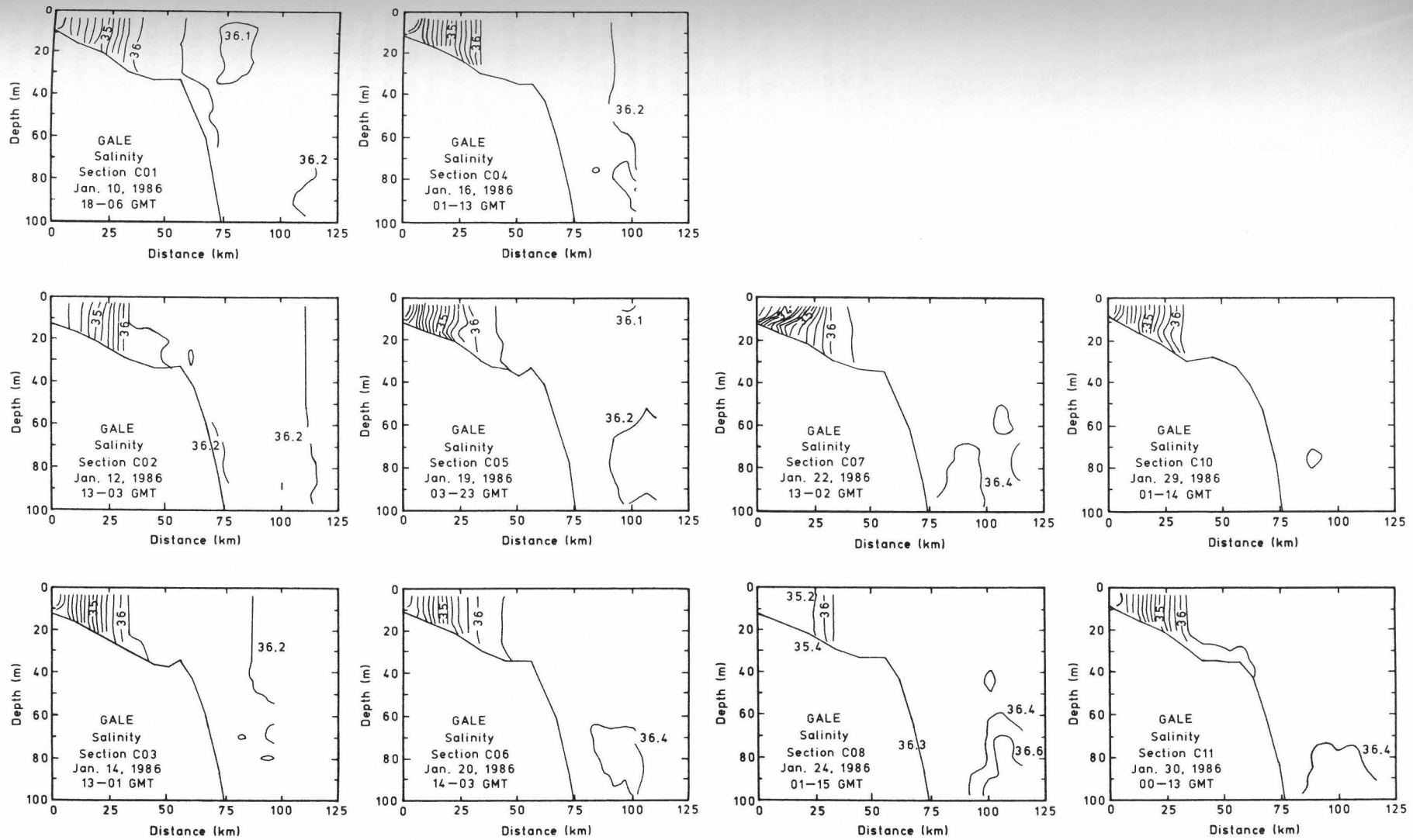

Fig. 6. Cross-shelf sections of salinity off Charleston.

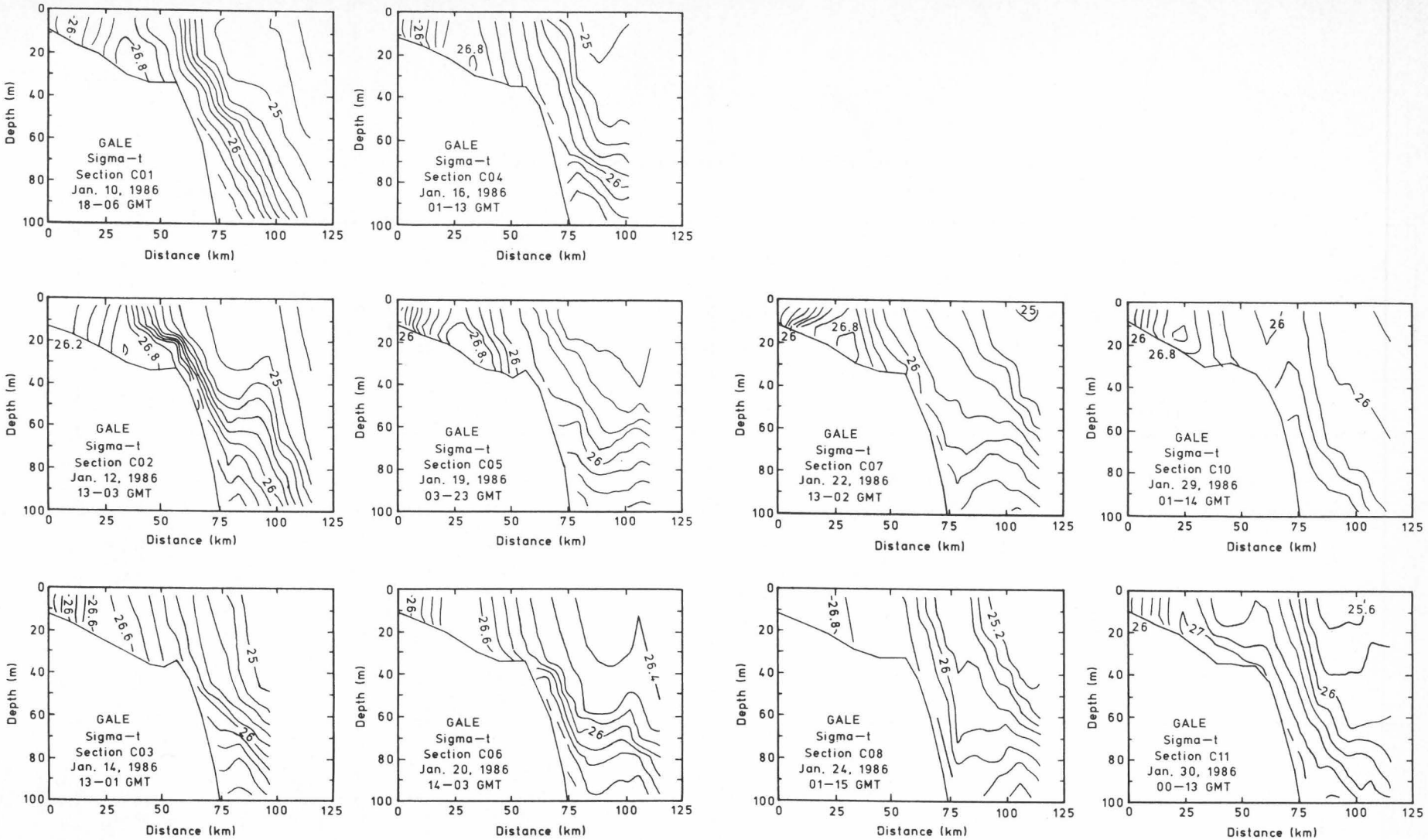

Fig. 7. Cross-shelf sections of density off Charleston.

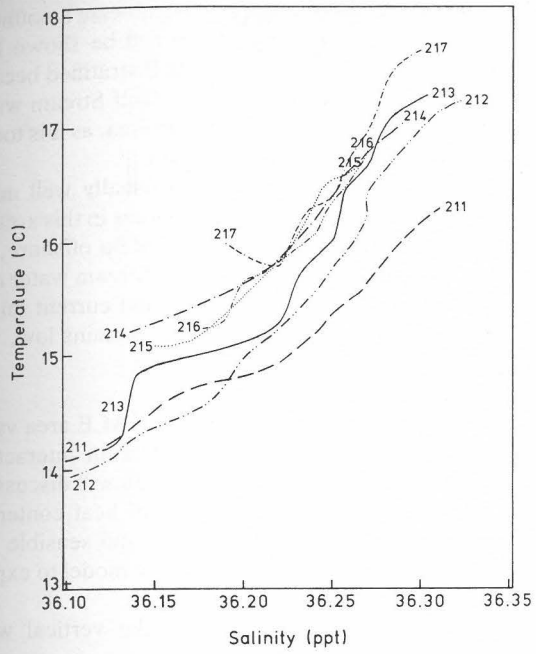

Fig. 8. *T-S* plot for stations 211–217 across the onshore intrusion event. Station 211 is nearshore, and station 217 is near the shelf break. The plot shows that deeper waters are fresher, suggesting offshore flow of cooled shelf waters.

as were the fluctuations in that area. The variability over the outer shelf and upper slope was complex with no obvious correlation between station locations. There was a trend for decreasing PE during the sampling period that may have been related to intensified mixing or the offshore movement of the Gulf Stream front. These stations are over the upper slope and shelf break where the Gulf Stream front is slightly tilted, where doming events were observed, and where onshore flow of surface water occurs during southward wind events.

Buoyancy Flux and Boundary Mixing

In this section buoyancy flux and mixing forces will be used to explain the observed temporal variation in stratification. Stratification in the SAB during the winter obviously seldom occurs. The strong winds, intense cooling, and shallow shelf waters all should preclude stratification. Nevertheless, stratification is observed occasionally.

The change in observed potential energy with time,

$$P_{\mathrm{PE}}^{\mathrm{OBS}} = \frac{\Delta\ \mathrm{PE}}{\Delta t} \qquad (\mathrm{W\ m^{-2}}) \tag{2}$$

expresses the net change in stratification because of all the buoyancy and mixing forces present. Those forces are the buoyancy flux including advective flux, wind mixing, and current mixing. A positive $P_{\mathrm{PE}}^{\mathrm{OBS}}$ shows increasing PE and stratification. $P_{\mathrm{PE}}^{\mathrm{OBS}}$ is what was observed by making repeated conductivity-temperature-depth (CTD) measurements at fixed locations across the shelf.

Buoyancy flux is a process that tends to stratify or mix the water column by varying the density of the water while wind energy at the surface and current energy on the bottom mix the water column. To compare these processes, one must define power densities that allow the direct comparison of buoyancy and mixing processes. The power required to negate buoyancy flux caused by air-sea heat transfer is heat buoyancy power density [*Atkinson and Blanton*, 1986]

$$P_Q = B\rho_w \frac{h}{2} \qquad (\mathrm{W\ m^{-2}}) \tag{3a}$$

and the power required to negate a buoyancy flux caused by advection is defined similarly as advective buoyancy power density

$$P_A = A\rho_w \frac{h}{2} \qquad (\mathrm{W\ m^{-2}}) \tag{3b}$$

where B is the buoyancy flux (modified from *Gill* [1982])

$$B = c_w^{-1} g \frac{\alpha}{\rho_w} (Q) \qquad (\mathrm{m^2\ s^{-3}}) \tag{4}$$

and

c_w specific heat of water (4000 J kg^{-1} °K^{-1});
g gravitational constant;
ρ_w water density;
h water depth;
α thermal expansion coefficient of seawater at the surface (2×10^{-4} °K^{-1});
Q measured heat flux (W m^{-2});
A advective buoyancy flux (m^2 s^{-3}).

The advective buoyancy flux A is an unknown but important quantity that will be determined.

The two processes that decrease potential energy by mixing the water column are wind and current. The wind power density is

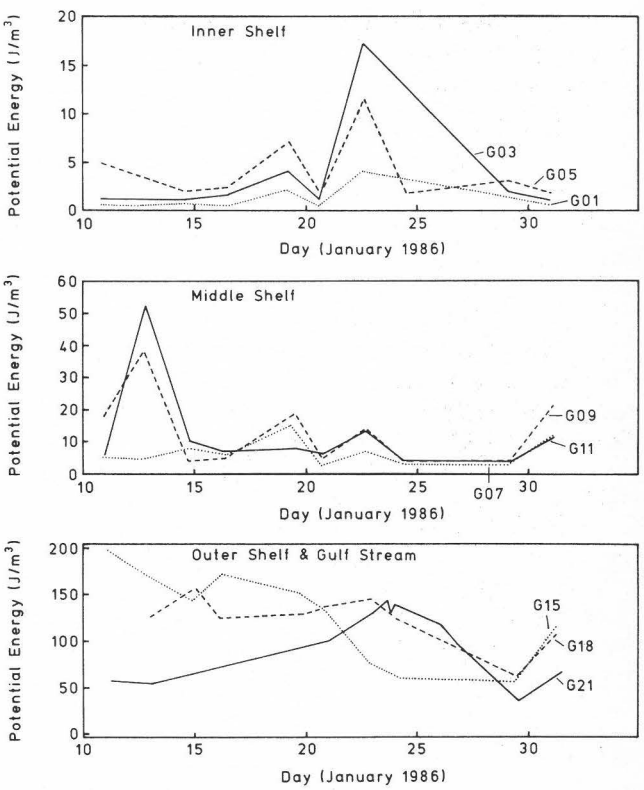

Fig. 9. Variability of potential energy at each hydrographic station: (top) inner shelf stations, (middle) middle shelf stations, (bottom) outer shelf and upper slope stations. Note Y axis scale change between panels. Increasingly negative PE indicates stratification, while increasingly positive PE indicates mixing.

$$P_w = \rho_w U_*^3 = \rho_w[(\rho_a/\rho_w)C_d]^{3/2}U_a^3 \qquad (\text{W m}^{-2}) \qquad (5)$$

where ρ_a are the densities of air, U_* is the friction velocity, U_a is the wind speed, and C_d is the drag coefficient (2×10^{-3}). Current power density is

$$P_C = \beta\rho_w C_d^{3/2} U_c^3 \qquad (\text{kg s}^{-3}) \qquad (6)$$

where β is an efficiency factor, typically 0.15 [*Fearnhead*, 1975], and U_c is the near-bottom current.

We can now equate these powers with the following relation:

$$P_{\text{PE}}^{\text{OBS}} = P_Q + P_A + P_W + P_C$$

P_W and P_C mix the water column, decreasing PE, while P_Q and P_A add buoyancy, increasing PE. In the following discussion, P_A will be determined, since $P_{\text{PE}}^{\text{OBS}}$, P_Q, P_W, and P_C can all be calculated from observations.

Two specific stratification events will be discussed, one over the inner shelf and one over the middle and outer shelf. The features of the two events are shown in Figure 10. Between January 10 and 12 the outer half of the shelf stratified during a period of southward wind accompanied by cooling in the presence of a small doming feature. Between January 20 and 22 the inner shelf stratified during a period of offshore winds also accompanied by cooling.

Inner shelf. The only time that the inner shelf stratified was on January 22 after a period of weak offshore winds and modest cooling. The power densities were calculated using the following values: winds, 8 m s^{-1}; currents 0.2 m s^{-1} at G01 and 0.1 m s^{-1} at G03 and G05; and heat flux (+350 W m^{-2}). $P_{\text{PE}}^{\text{OBS}}$ was determined from CTD observations at stations G01, G02, and G03 on the two dates. Since P_c was several orders of magnitude less than the other terms, it is not included. Table 1 shows the results. The PE always increased (the water column stratified), and $P_{\text{PE}}^{\text{OBS}}$ was positive. This occurred in spite of P_W and P_Q (cooling) that decrease PE. The only source of such buoyancy to increase PE is via the advection of buoyancy from nearshore. The last column represents the amount of advective buoyancy flux in terms of power density that is needed to produce the observed stratification considering the amount of energy available. The important point here is that the power density related to advective buoyancy flux is greater than any other buoyancy creation or destruction process. The only source for this is the offshore transport of low-salinity water. The values of P_A convert to about 0.05 m H_2O m^{-2} month^{-1} of runoff, a value that is low compared with long-term means [*Atkinson and Blanton*, 1986] but within the same order.

Outer shelf. The outer half of the shelf became stratified between January 10 and 12. The power densities and change in PE were calculated by the same procedure as with the inner shelf event. The values used were as follows: wind was 8 m s^{-1}, and air-sea heat flux was 260 W m^{-2} at G07, 370 W m^{-2} at G09, and 500 W m^{-2} at G11. Heat flux was estimated from data in Figure 10. Since latent heat flux was not calculated, the total heat flux was estimated from the January 20 and 21 sections to be about 4 times the sensible heat flux. Power density related to current (P_C) was again orders of magnitude less than other power densities and was not calculated.

As is shown in Table 2, the outer shelf PE increased, and stratification occurred again in spite of significant amounts of energy available for decreasing PE. It will be shown later that during this time period the outer shelf stratified because of Ekman-driven onshore flow of warm Gulf Stream water. This is the only source of buoyancy in the area, as it is too far offshore to receive buoyant coastal water.

Middle shelf. The middle shelf was usually well mixed ($P_{\text{PE}}^{\text{OBS}} \sim 0$). This is because buoyancy sources in this area are small. Runoff normally does not extend that far offshore, and the onshore flow of buoyant surface Gulf Stream water does not extend this far onshore. Thus wind and current mixing and cooling prevail, and middle shelf PE remains low.

A Model of Heat Content Variability

The heat content of shelf waters in the GALE area varies because of air-sea heat flux and Gulf Stream interaction, both of which are considerable. This section will discuss the observed temporal and spatial variation of heat content of the water column, compare it with latent and sensible heat flux at the sea surface, and present a simple model to explain the variability.

The heat content (per unit area) of the vertical water column is

$$H(t) = C_p\rho \int_{-h}^{0} T\, dz = C_p\rho h\bar{T} \qquad (\text{J m}^{-2}) \qquad (7)$$

where $C_p\rho$ is taken as a constant ($\approx 4 \times 10^6$ J m^{-3} °K^{-1}) and $\bar{T}$ is depth-averaged temperature. As a first test, the idea that the observed temporal variation of water column heat content in inner shelf waters (G01 for example) depends solely on air-sea heat flux (advective effects are minimal) is examined. The temporal variation of heat content due only to surface heat flux is

$$H_Q(t) = H(t_0) - \int_{t_0-\Delta\tau}^{t-\Delta\tau} (Q_C + Q_E + Q_S)\, dt \qquad t \geq t_0 \qquad (8)$$

where Q_C is the observed sensible heat loss, Q_E is the observed latent heat loss, Q_S is the monthly mean incident short wave solar radiation, and t_0 is the initial time. $\Delta\tau$ is a time lag that approximately models the finite mixing time of the water column and is $O(h^2/K_H)$, where K_H is vertical eddy diffusivity and is about $(\tau/\rho)^{1/2}h/20$ with $\tau \approx 0.1\ P$ and $h \approx 10$ m, K_H is $O(10^{-3}$ m^2 s$^{-1})$ and $\Delta\tau$ is $O(1$ day). $H(t)$ versus $H_Q(t)$ is shown in Figure 11. The Q_C and Q_E values were calculated from observations at the Savannah navigational light tower (SNLT). Q_S was estimated to be 40 W m^{-2}. Since the other heating terms are 5 times larger than Q_S, an error in Q_S is insignificant. The comparison between the observed change in heat content, $H(t)$, and the calculated change, $H_Q(t)$, were close, suggesting that the advective effects were minimal. The discrepancy between the two should be attributed to the possibility of advective heat fluxes in the coastal area and uncertainty in the heat flux terms.

Next, the cross-shelf variation of heat content is considered and compared with calculated surface heat flux. The temporal variation of H at each station is calculated by the difference of $\bar{T}$ of two successive hydrographic observations of which the time difference, Δt, is about 2 days an average. The heat flux $\Delta H \equiv dH/dt$ is then obtained by

$$\Delta H = C_p\rho h \frac{\Delta\bar{T}}{\Delta t} \qquad (\text{W m}^{-2}) \qquad (9)$$

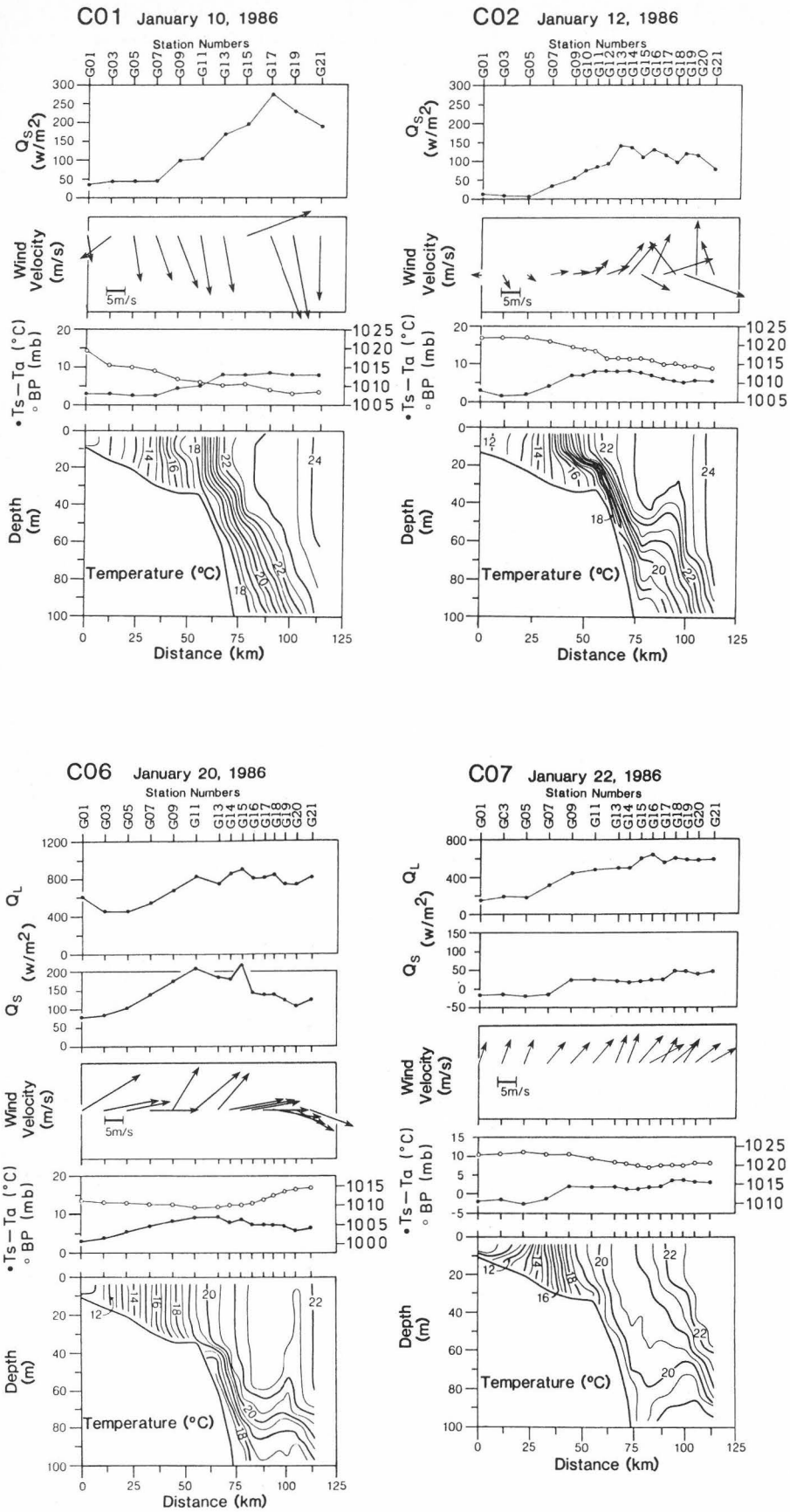

Fig. 10. Vertical sections, winds and heat flux across the shelf during inner and outer shelf stratification events.

TABLE 1. Power Density Values for the January 20–22 Inner Shelf Stratification Event

Station	Depth, m	ΔPE	ΔT	P_{PE}^{OBS}	P_W	P_Q	P_A
G01	10	42	1.7×10^5	0.2	1.5	−0.8	2.5
G03	15	260	1.7×10^5	1.5	1.5	−1.3	4.3
G05	20	210	1.7×10^5	1.2	1.5	−1.7	4.4

P values are in milliwatts per square meter.

ΔH is evaluated spatially at each station from G01 to G19 and temporally from January 10 to 30 for 10 cases. The results are plotted along the section line from onshore to offshore in Figure 12 with the values of $-(Q_C + Q_E)$ for comparison. Two main features of the figure are clear. The heat flux at inner stations (G01–G05) was low in magnitude and variation, while the outer stations' heat flux was large in magnitude and variation. Surface heat flux based on Q_C and Q_E was less variable compared with observed water column heat variations. At inner stations, $-(Q_C + Q_E)$ agrees well with ΔH, supporting the idea that inner shelf heat budget may be obtained by a balance with surface heat flux only [*Oey*, 1986] and that Gulf Stream interaction with outer shelf water is an important process in the outer shelf region [*Oey et al.*, 1987].

To separate the effects of air-sea interaction, Gulf Stream meanders, and onshore Ekman flow from the Gulf Stream, the simple box model shown in Figure 13 is used. The box covers the continental shelf region with unit along-shore width. The horizontal distance, L, spans about 56 km (from station G01 to station G11). The rate of change of the heat content of the continental shelf box is

$$\Delta H = \Delta H_E - \Delta Q + \Delta H_{GS} \tag{10}$$

where ΔH_E is heat flux by Ekman flow, ΔQ is air-sea heat flux over the shelf area, ΔH_{GS} is heat flux by Gulf Stream meanders, and ΔH is the observed heat content variation in the box.

If cross-shore transport at G01 is assumed null, ΔH_E is given by

$$\Delta H_E = C_p \rho (U_i T_i - U_o T_o + V_i T_m - V_o T_m) \tag{11}$$

Equation (11) relates the ΔH_E to advective alongshore transports ($V_i T_m$, $V_o T_m$) and cross-shelf transports ($U_i T_i$, $U_o T_o$). To close this equation, we state that the cross-shelf U_o is a proportion (not necessarily fixed) of U_i, or $U_o = nU_i$. Using this and continuity of volume

$$V_i - V_o + U_i - U_o = 0$$

equation (11) becomes

$$\Delta H_E = C_p \rho U_i [T_i - T_m + n(T_m - T_o)] \tag{12}$$

TABLE 2. Power Density Values for the January 10–12 Outer Shelf Stratification Event

Station	Depth, m	ΔPE	ΔT	P_{PE}^{OBS}	P_W	P_Q	P_A
G07	30	0.0	1.5×10^5	0	−1.5	−1.9	≤3.4
G09	34	1200	1.5×10^5	8.0	−1.5	−3.1	13
G11	34	1600	1.5×10^5	10.7	−1.5	−4.1	16

P values are in milliwatts per square meter.

where U_i, U_o, V_i, V_o, T_i, T_o, and T_m are the inflow and outflow transports, alongshore inflow and outflow transports, and the water temperatures. T_i, T_o, and T_m were determined to be 19°C, 18°C, and 13°C, respectively, from the mean surface and bottom temperatures at the shelf break and the mean temperature of the entire shelf during the GALE observations. The number n is a fraction of the inflow U_i flowing offshore with the remainder $(1-n)$ flowing alongshore. The onshore Ekman transport, U_i, is calculated from the alongshore wind stress τ_y,

$$U_i = \frac{\tau_y}{\rho f} \quad (\mathrm{m^2\ s^{-1}}) \tag{13}$$

with southward wind stress, τ_y, positive so the surface inflow is positive. Wind stress for this calculation was determined from the hourly recorded data for the past 3 days from the date considered. The time lag was estimated by the advective time of Ekman flow over a horizontal distance of $O(10$ km), i.e.,

$$O(t) = O(L) \Big/ \left[O\left(\frac{\tau_y}{\rho f h} \right) \right]^{-1}$$

$$= 10^4 \Big/ \left(\frac{0.1}{10^3 \times 10^{-4} \times 30} \right)^{-1} \approx 3 \text{ days} \tag{14}$$

Using (10), (11), (12), and (13), ΔH and ΔH_E were calculated for dates at the midpoint of two successive hydrographic stations with ΔH_E obtained by averaging 3-day wind data before that date. The constant value ΔQ was -275 W m^{-2}, obtained from the mean surface heat flux, $\overline{Q}_S + \overline{Q}_L$ (-78 and -197 W m^{-2}) by integrating over the shelf and over the GALE period. The resultant ten calculations in January (11.8, 13.7, 15.6, 17.9, 20, 21.7, 23.6, 25.1, 27.5, and 30.2, in decimal days) of ΔH versus $-\Delta H_E$ are shown in Figure 14. The number n (equation (12)) was determined by maximizing the correlation between ΔH and ΔH_E. The best correlation of the two variables was obtained with $n = 0.1$, where 90% of the inflow is lost by divergence in shelf waters. The dotted line represents the correlation between ΔH and ΔH_E with ΔQ set at -275 W m^{-2} where the observed heat variability depends solely on air/sea heat exchange and Ekman transport. Since the data fall reasonably close to the line it is concluded that shelf water heat content does indeed depend to a large extent on Ekman transport.

Deviations of observations from the line represent contributions to the heat content variability by Gulf Stream eddies

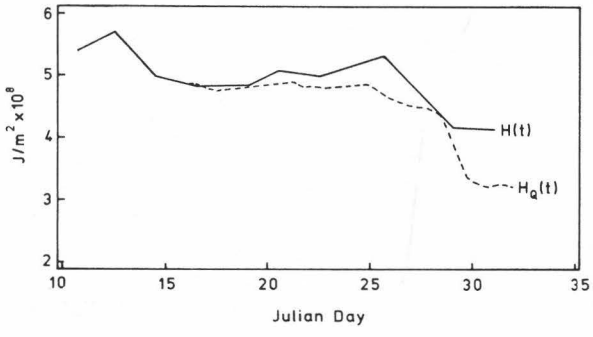

Fig. 11. Time-integrated heat flux calculated from hydrographic observations at station G01 ($H(t)$) compared with latent and sensible heat fluxes calculated from meteorological observations at the Savannah navigational light tower ($H_Q(t)$).

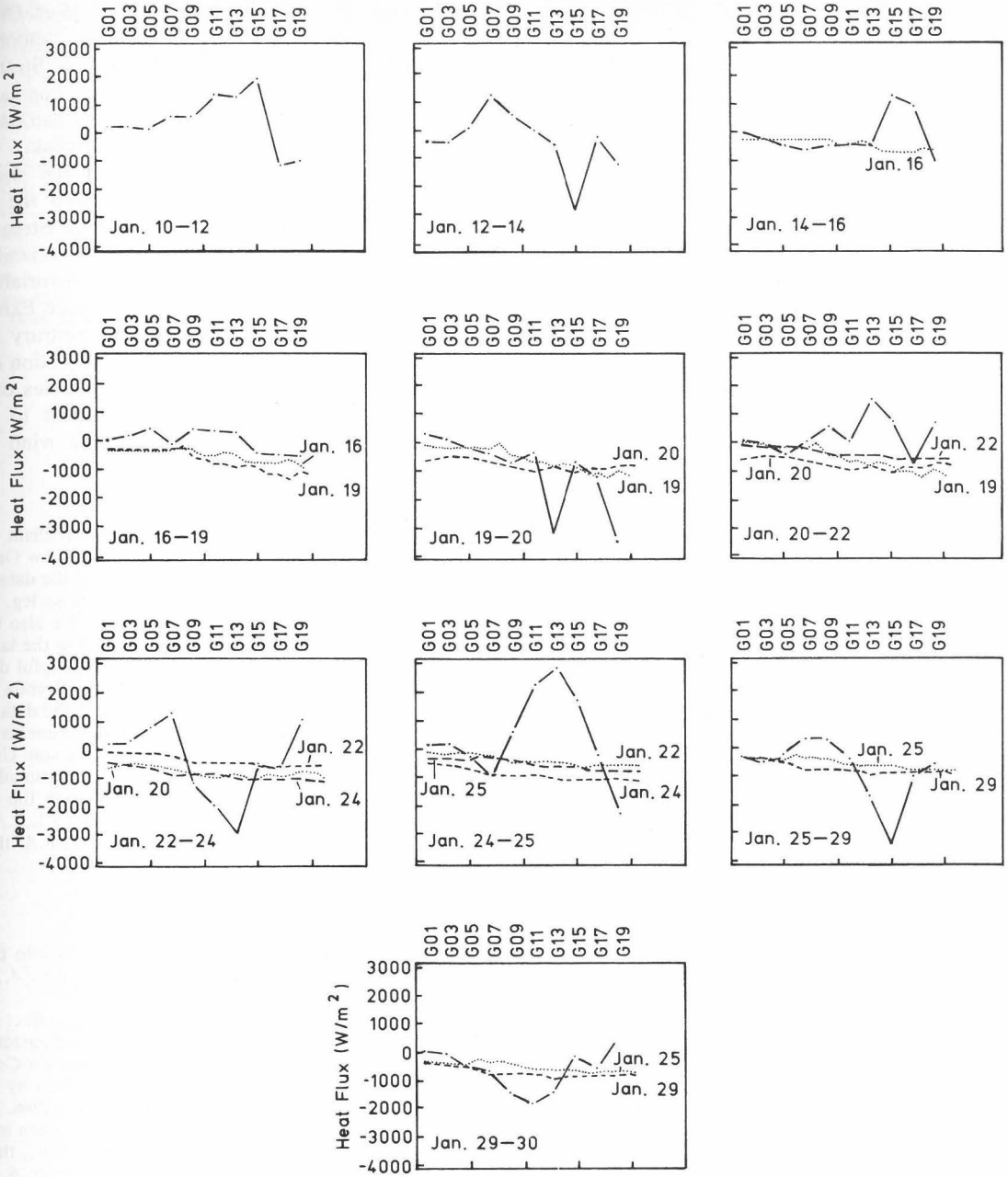

Fig. 12. Heat flux calculated from observed changes in heat content at hydrographic stations (long dash–dot line) compared to "instantaneous" heat flux calculated for meteorological observations taken on board the ship (short-dashed and dotted lines). The date on lower part of each panel gives the 2 days used for the heat flux based on hydrographic observations. The data beside the finer short-dashed lines and the dotted lines indicate the heat flux based on meteorological observations of that day.

and meanders and other effects. There was evidence of a Gulf Stream eddy during the GALE period. It appeared in the area south of the section of January 11–17 and passing by on January 18–24. Four of the five data points (January 17, 21, 23, and 27) that deviate greatly from the line are during this period of eddy-meander activity. The effect of eddy-meander activity on the shelf heat balance, ΔH_{GS}, can be estimated from those four values and is about 300 W m^{-2}. The Gulf Stream appears to be warming the shelf on January 17–23 (except January 20) and cooling on January 25–27, which is consistent if the Gulf Stream was passing through the area on January 18–24. The model suggests that the heat flux into shelf waters was due to Ekman and eddy-meander flow over the shelf break. This advective heat flux from the Gulf Stream represents the advective buoyancy flux that was determined indirectly in the section of buoyancy flux/potential energy. In that section it was found that variation in shelf PE depended as much or more on buoyancy advection as on air-sea heat exchange. If the conceptual model is correct, the advective buoyancy flux should be equivalent to $\Delta H_E + \Delta H_{GS}$. This can be tested with the January 10–12 data. The calculated Ekman heat flux (ΔH_E) on January 11 was 700 W m^{-2}, and the Gulf Stream component was zero (Figure 14). This converts to equivalent buoyancy power density by successive use of equations (4) and (3) to 5 m W m^{-2} that is of the same range as the observed P_A values in

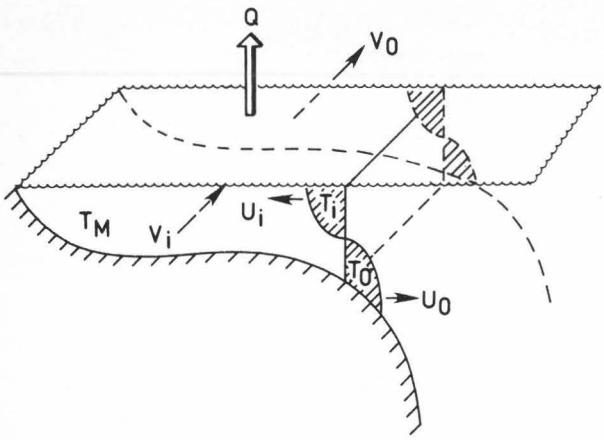

Fig. 13. Schematic of the model used to test the hypothesis that the variability of heat content observed in shelf waters depends on onshore Ekman flow of warm Gulf Stream water. T_i and T_o are the average temperature of the upper and lower layers over the whole period. $H(t)$ is the observed heat content. Q is the estimated heat exchange from measurements at SNLT. V_i and V_o are the calculated Ekman transports in the upper and lower layer. U_i and U_o are the onshore velocities in the upper layer and offshore velocities in the lower layer.

Table 2 (3–16 m W m^{-2}). This further confirms the hypothesis that variation in PE and stratification over the outer shelf are controlled by intrusions of Gulf Stream water under the influence of either the wind or Gulf Stream meanders.

Conclusion

The observations made during the GALE experiment were some of the first to document the response of a wide, shallow shelf area and adjacent boundary current to intense winter winds and cooling.

Stratification over the shelf and the position of the fronts were significantly affected by the advection of buoyancy. During stratification events over the inner shelf, advection of buoyancy was 1 to 3 times higher than mixing processes. Over the outer shelf, it was up to 4 times higher. Of course, the shelf was well mixed much of the time, demonstrating the effectiveness of wind mixing and heat loss. Stratification occurred only when winds moved buoyant coastal waters offshore or Gulf Stream waters inshore, or when eddies and meanders advected water across the shelf break.

The observations of heat variation on the shelf were explained by using a model that estimated the relative contribution of Gulf Stream meanders, Gulf Stream intrusions, and Ekman transport to the observed variability. The simple models showed that the observed heat variability and stratification are caused mostly by the onshore Ekman flow of warmer Gulf Stream water. This is contrary to most stratification models that do not include advection of buoyancy. This study clearly shows that any studies of middle and outer shelf processes in areas adjacent to western boundary currents must consider both the wind and the boundary current.

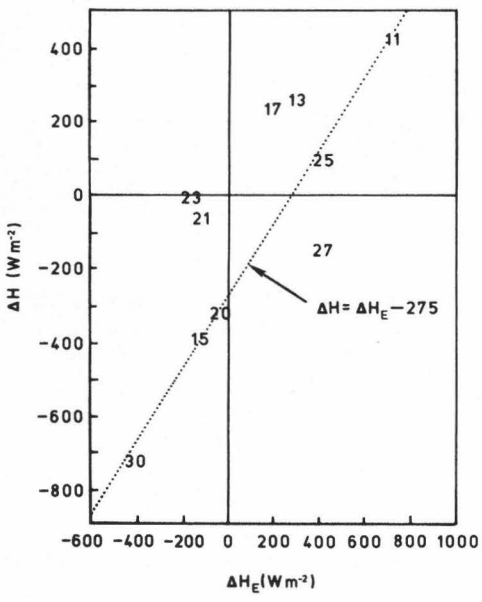

Fig. 14. Plot of observed heat flux (ΔH) versus heat flux caused by onshore Ekman flux (ΔH_E).

Acknowledgments. We would like to thank William Chandler and Tad Guy for their assistance. We thank Lie-Yauw Oey for the considerable time he gave to the interpretation of the data, William Dunstan for serving as Chief Scientist on one cruise leg, and John Bane for stimulating discussion and comments. We also thank the other GALE participants who helped at sea and in the laboratory. The crew of the R/V *Endeavor* were especially helpful during the stormy expedition. Julie Amft, Patmarie Maher, Brenda Norman, and Kathryn Bush are thanked for their help with the data analysis. Computing resources were provided by the departments of Computer Sciences and Oceanography at Old Dominion University. Funding for this study was provided by the National Science Foundation and the Department of Energy through the following grants: OCE-8519203 and DE-FG05-85ER60348 to L.P.A., OCE-8516132 to T.N.L., and OCE-8516129 to J.O.B. L.P.A. thanks the Smith Foundation for partial salary support.

References

Atkinson, L. P., Modes of Gulf Stream intrusion into the South Atlantic Bight shelf waters, *Geophys. Res. Lett.*, *4*, 583–586, 1977.

Atkinson, L. P., and J. O. Blanton, Processes that affect stratification in shelf waters with examples from the southeastern United States continental shelf in *Baroclinic Processes on Continental Shelves*, *Coastal and Estuarine Sci.*, vol. 3, edited by C. N. K. Mooers, pp. 117–130, AGU, Washington, D. C., 1986.

Bane, J. M., Jr., and K. E. Osgood, Wintertime air-sea interaction processes across the Gulf Stream, *J. Geophys. Res.*, this issue.

Blanton, J. O., T. N. Lee, L. P. Atkinson, J. M. Bane, A. Riordan, and S. Raman, Oceanographic studies during Project GALE, *Eos Trans. AGU*, *68*, 1626–1637, 1987.

Blanton, J. O., J. A. Amft, D. K. Lee, and A. Riordan, Wind stress and heat fluxes observed during winter and spring 1986, *J. Geophys. Res.*, this issue.

Fearnhead, P. G., On the formation of fronts by tidal mixing around the British Isles, *Deep Sea Res.*, *22*, 311–321, 1975.

Garwood, R. W., R. Fett, K. Rabe, and H. Brandli, Ocean frontal formation due to shallow water cooling effects as observed by satellite and simulated by a numerical model, *J. Geophys. Res.*, *86*, 11,000–11,012, 1981.

Gill, A. E., *Atmosphere-Ocean Dynamics*, 662 pp., Academic, San Diego, Calif., 1982.

Huh, O. K., W. J. Wiseman, and L. J. Rouse, Jr., Winter cycle of sea surface thermal patterns, northeastern Gulf of Mexico, *J. Geophys. Res.*, *83*, 4523–4529, 1978.

Huh, O. K., L. J. Rouse, Jr., and N. D. Walker, Cold air outbreaks over the northwest Florida continental shelf: heat flux process and hydrographic changes, *J. Geophys. Res.*, *89*, 717–726, 1984.

Lee, T. N., E. Williams, J. Wang, R. Evans, and L. Atkinson, Response of South Carolina continental shelf waters to wind and Gulf Stream forcing during winter of 1986, *J. Geophys. Res.*, this issue.

Nowlin, W. D., and C. A. Parker, Effects of cold-air outbreak on shelf waters of the Gulf of Mexico, *J. Phys. Oceanogr.*, *4*, 467–486, 1974.

Oey, L., The formation and maintenance of density fronts on the U.S. southeastern continental shelf during the winter, *J. Phys. Oceanog.*, *16*, 1119–1133, 1986.

Oey, L.-Y., L. P. Atkinson, and J. O. Blanton, Shoreward intrusion of upper Gulf Stream water onto the U.S. southeastern continental shelf, *J. Phys. Oceanogr.*, *17*, 2318–2333, 1987.

Price, J. E., C. N. K. Mooers, and J. C. Van Leer, Observations and simulation of storm-induced mixed layer deepening, *J. Phys. Oceanogr.*, *8*, 582–599, 1978.

Stefansson, U., L. P. Atkinson, and D. F. Bumpus, Hydrographic properties and circulation of the North Carolina shelf and slope waters, *Deep Sea Res.*, *18*, 383–420, 1971.

L. P. Atkinson, E. Oka, and S. Y. Wu, Department of Oceanography, Old Dominion University, Norfolk, VA 23529.

T. J. Berger, Science Applications International Corporation, 4900 Waters Edge Road, Suite 255, Raleigh, NC 27606.

J. O. Blanton, Skidaway Institute of Oceanography, P.O. Box 13687, Savannah, GA 31426.

T. N. Lee, Rosenstiel School of Marine and Atmospheric Science, University of Miami, 4600 Rickenbacker Causeway, Miami, FL 33149.

(Received June 28, 1988;
accepted September 5, 1988.)